Schrödinger optical-potential calculation of 500 MeV polarized proton scattering from polarized ^{13}C

T. Mefford and R.H. Landau
Physics Department, Oregon State University, Corvallis, Oregon

L. Berge and K. Amos
School of Physics, University of Melbourne, Parkville, Victoria 3052, Australia
(Received 13 May 1994)

Spin observables for elastic p-^{13}C scattering at 500 and 547 MeV are calculated using a microscopic, momentum-space optical potential in a relativistic Schrödinger equation. Included are the full spin dependences, off-energy-shell kinematics and dynamics, several models for the nuclear structure, exact treatment of the Coulomb force, and spin singlet-triplet mixing. Agreements with data are good for some observables but, in other observables, indicate the need for additional physics.

PACS number(s): 24.10.Ht, 24.70.+s, 25.10.+s, 25.40.Cm

I. INTRODUCTION

Recent experimental advances have combined polarized nuclear targets with polarized proton beams to measure more and more of the 36 possible spin observables describing the elastic scattering of two spin-1/2 particles [1–4]. Most of these observables have never been measured before at intermediate energies, and it is of basic interest to understand what aspects of nuclear spin dynamics may be revealed by them. This is a challenging problem because, on the one hand, the connection between an observable and dynamics is often not direct [5], and, on the other hand, a spin observable often arises from delicate interferences within the scattering amplitude. Accordingly, it is not surprising to find a theory that is fine for predicting differential cross sections and analyzing powers has problems with the spin observables.

In the present work we report on a microscopic, optical-potential calculation of polarized-proton scattering from a polarized ^{13}C nucleus. We use a microscopic, first-order potential in momentum space, including the full spin structure of the proton-nucleon and proton-carbon interactions, spin singlet-triplet mixing, and an exact treatment of the Coulomb potential via an extension of the Vincent-Phatak matching procedure. We solve a relativistic Lippmann-Schwinger equation and make comparisons to available data near 500 MeV. While we find good agreement between our predictions and experiment for some observables, we also find poor agreement, for no apparent reason, with others.

As part of the present work we have extended the Stapp phase-shift analysis of nucleon-nucleon scattering [6,7] to the more general case of nonidentical spin-1/2 particles in the angular momentum basis. The requisite coupling of the spin singlet and triplet channels is equivalent to including isospin-symmetry breaking effects in the NN problem. Related extensions have been made by Gersten *et al.* [8] in the helicity basis with specialization to one-boson exchange potentials, and by Williams *et al.* [9] in Born approximation.

In contrast to the full solutions of the p-^{13}C Lippmann-Schwinger equation reported here, the calculations by Seestrom-Morris *et al.* [1], Ray *et al.* [2], Hoffmann *et al.* [3], and Hoffmann *et al.* [4] are based on a relativistic distorted wave impulse approximation (DWIA). While the basic physics in the impulse approximation and optical potential is similar, cancellation effects and the large number of partial waves involved make the predictions sensitive to the theoretical differences. On a more phenomenological level, the DWIA studies first adjust the optical potential to obtain a best fit to the p-^{12}C scattering data, and then use the corresponding distorted wave to predict p-^{13}C scattering. Our calculations, in contrast, are independent of p-^{12}C scattering data, contain different multiple scattering processes, use different assumptions for off-energy-shell kinematics and dynamics, and, although relativistic, contain no negative-energy degrees of freedom.

II. SPIN PHENOMENOLOGY

The p-^{13}C spin $1/2 \times 1/2$ elastic scattering observables all derive from a T matrix which has a spin-space structure much like that for the NN system. If we assume rotation invariance, parity conservation, and time reversal invariance, this structure is [6,10–12]

$$2\,T(\mathbf{k}',\mathbf{k}) = a + b + (a-b)\vec{\sigma}_n^p\vec{\sigma}_n^C + (c+d)\vec{\sigma}_m^p\vec{\sigma}_m^C + (c-d)\vec{\sigma}_l^p\vec{\sigma}_l^C + e(\vec{\sigma}_n^p + \vec{\sigma}_n^C) + f(\vec{\sigma}_n^p - \vec{\sigma}_n^C), \tag{1}$$

where we have suppressed the $(\mathbf{k}',\mathbf{k})$ dependence of a–f. The superscripts "p" and "C" in Eq. (1) indicate the projectile and target, respectively, while the subscripts indicates a dot product of σ with one of the three independent unit vectors:

$$\hat{\mathbf{n}} = \frac{\mathbf{k}\times\mathbf{k}'}{|\mathbf{k}\times\mathbf{k}'|}, \quad \hat{\mathbf{m}} = \frac{\mathbf{k}-\mathbf{k}'}{|\mathbf{k}-\mathbf{k}'|}, \quad \hat{\mathbf{l}} = \frac{\mathbf{k}+\mathbf{k}'}{|\mathbf{k}+\mathbf{k}'|}, \tag{2}$$

where the vectors $\mathbf{k}$ and $\mathbf{k}'$ are the incident and scattered proton momenta in the c.m. frame and define the scattering plane. The vector $\hat{\mathbf{n}}$ is *normal* to the scattering plane, the vector $\hat{\mathbf{m}}$ is in the scattering plane along the *momentum* transfer $\mathbf{q} = \mathbf{k}' - \mathbf{k}$ direction (*sideways* to the beam direction), and $\hat{\boldsymbol{l}}$ is in the scattering plane (*longitudinal* to the beam direction). For on-shell ($k' = k$) scattering, the vectors $\hat{\boldsymbol{l}}$ and $\hat{\mathbf{m}}$ are orthogonal.

In terms of conventional nuclear forces, the $(a+b)$ term in Eq. (1) arises from a "central" force, the e and f terms from "spin-orbit" forces, and $(a-b)$, $(c+d)$, and $(c-d)$ from "tensor" forces. In NN scattering the particles are identical, and if the generalized exclusion principle (including isospin) holds true, the f term vanishes. In p-^{13}C scattering, no symmetry principle forbids f and this results in the spin singlet and triplet states being coupled.

There are 36 spin observables for the scattering of two spin-1/2 particles which can be formed from the amplitudes in Eq. (1) [10,11,13] The observables recently measured [1,3,4] are related to the amplitudes in Eq. (1) by

$$\frac{d\sigma^{(1)}}{d\Omega} = \frac{1}{2}(|a|^2 + |b|^2 + |c|^2 + |d|^2 + |e|^2 + |f|^2), \tag{3}$$

$$A^{(2)}_{oono} = \frac{1}{\sigma}\mathrm{Re}(a^* e + b^* f), \tag{4}$$

$$A^{(2')}_{ooon} = \frac{1}{\sigma}\mathrm{Re}(a^* e - b^* f), \tag{5}$$

$$D^{(3)}_{nono} = \frac{1}{2\sigma}(|a|^2 + |b|^2 - |c|^2 - |d|^2 + |e|^2 + |f|^2), \tag{6}$$

$$D^{(4)}_{loso} = \frac{1}{\sigma}\mathrm{Im}(b^* e + a^* f), \tag{7}$$

$$D^{(5)}_{soso} = \frac{1}{\sigma}\mathrm{Re}(a^* b + c^* d - e^* f), \tag{8}$$

$$A^{(11)}_{oonn} = \frac{1}{2\sigma}(|a|^2 - |b|^2 - |c|^2 + |d|^2 + |e|^2 - |f|^2). \tag{9}$$

Here we use the traditional Wolfenstein notation as analyzing powers, polarizations, and depolarizations, as well as the tensor notation $X^{(n)}_{p't'pt}$ with the subscripts p and t denoting the direction of the initial-state projectile and target polarizations, the primes denoting the corresponding final-state quantities, and a subscript o signifies zero or undetected polarization. The superscript (n) refers to the variable number that is tabulated in [13], a redundancy we find useful when dealing with difficult-to-pronounce and easy-to-confuse variables.

III. OPTICAL POTENTIAL

Our theoretical input is a microscopic, first-order, momentum-space optical potential [13,15,16]:

$$\begin{aligned} V(\mathbf{k}',\mathbf{k}) \simeq\ & N\left\{(t^{pn}_{a+b} + t^{pn}_{e}\vec{\sigma}^{p}_{n})\rho^{n}_{\mathrm{mt}}(q)\right. \\ & \left. + \left[t^{pn}_{a-b}\vec{\sigma}^{p}_{n}\vec{\sigma}^{C}_{n} + t^{pn}_{e}\vec{\sigma}^{C}_{n} + t^{pn}_{c+d}\vec{\sigma}^{p}_{m}\vec{\sigma}^{C}_{m} + t^{pn}_{c-d}\vec{\sigma}^{p}_{l}\vec{\sigma}^{C}_{l} + t^{pn}_{c+d}(\vec{\sigma}^{p}_{m}\vec{\sigma}^{C}_{l} + \vec{\sigma}^{p}_{l}\vec{\sigma}^{C}_{m})\right]\rho^{n}_{\mathrm{sp}}(q)\right\} \\ & + Z\left\{(t^{pp}_{a+b} + t^{pp}_{e}\vec{\sigma}^{p}_{n})\rho^{p}_{\mathrm{mt}}(q)\right. \\ & \left. + \left[t^{pp}_{a-b}\vec{\sigma}^{p}_{n}\vec{\sigma}^{C}_{n} + t^{pp}_{e}\vec{\sigma}^{C}_{n} + t^{pp}_{c+d}\vec{\sigma}^{p}_{m}\vec{\sigma}^{C}_{m} + t^{pp}_{c-d}\vec{\sigma}^{p}_{l}\vec{\sigma}^{C}_{l} + t^{pp}_{c+d}(\vec{\sigma}^{p}_{m}\vec{\sigma}^{C}_{l} + \vec{\sigma}^{p}_{l}\vec{\sigma}^{C}_{m})\right]\rho^{p}_{\mathrm{sp}}(q)\right\} \qquad (10) \\ \stackrel{\mathrm{def}}{=}\ & \frac{1}{2}\left[V_{a+b}(\vec{k}',\vec{k}) + V_{a-b}(\vec{k}',\vec{k})\vec{\sigma}^{p}_{n}\vec{\sigma}^{C}_{n} + V_{c+d}(\vec{k}',\vec{k})\vec{\sigma}^{p}_{m}\vec{\sigma}^{C}_{m}\right. \\ & \left. + V_{c-d}(\vec{k}',\vec{k})\vec{\sigma}^{p}_{l}\vec{\sigma}^{C}_{l} + V_{e}(\vec{k}',\vec{k})(\vec{\sigma}^{p}_{n} + \vec{\sigma}^{C}_{n}) + V_{f}(\vec{k}',\vec{k})(\vec{\sigma}^{p}_{n} - \vec{\sigma}^{C}_{n})\right], \qquad (11) \end{aligned}$$

where the subscripts on t indicate their origins in terms of the elementary NN amplitudes. This potential manifestly contains the spin $1/2 \times 1/2$ dependence of nucleon-nucleon scattering weighted by four, possibly different, form factors describing the distributions of spin (sp) and matter (mt) for point protons and neutrons within the nucleus. The finite size of the nucleon is included in the pN t matrices, and thus must be removed from the form factors. To improve upon this theory one could include antisymmetrization of the projectile nucleon with the unstruck nucleons in the nucleus, NN correlations within the nucleus, intermediate nuclear excitations, Dirac-like relativity, and meson or quark currents.

If the charge and magnetic form factors of the mirror nuclei ^{13}C and ^{13}N were known, if isospin were a perfect symmetry, and if we could remove the meson-exchange currents from the electromagnetic form factors, then we could deduce the strong interaction form factors from these electromagnetic ones. While such is the case for the three-nucleon system, it is not yet possible for the 13-nucleon system. Instead we assume an independent particle shell model description of ^{13}C as a $1p_{\frac{1}{2}}$ valence neutron outside of a ^{12}C core of closed $1s_{\frac{1}{2}}$ and $1p_{\frac{3}{2}}$ shells. While it is known that the ^{12}C core is not spherical, and that core excitations play an important role in reactions with ^{12}C, we remain consistent with the assumptions of a first-order optical potential that ignores virtually excited intermediate states. For a harmonic-oscillator shape for the nucleus [17], the corresponding form factors are

$$\rho^{p}_{\mathrm{mt}}(r) = \rho_0\left[1 + \frac{N-2}{3}\frac{r^2}{a^2}\right]e^{-r^2/a^2}, \tag{12}$$

$$\rho^p_{\rm mt}(q) = \left[1 - \frac{Z-2}{6}q^2a^2\right] \frac{e^{-q^2a^2/4}}{f(q)}, \quad \rho^p_{\rm sp}(q) = 0, \tag{13}$$

$$\rho^n_{\rm sp}(q) = \left[1 - \frac{q^2a^2}{6}\right] \frac{e^{-q^2a^2/4}}{3Nf(q)}, \tag{14}$$

$$\rho^n_{\rm mt} = \left[1 - \frac{(N-2)q^2a^2}{6}\right] \frac{e^{-q^2a^2/4}}{f(q)} e^{-q^2a^2/4}, \tag{15}$$

$$f(q) = \left(1 + q^2/18.2\ \text{fm}^{-2}\right)^{-2}, \quad a = 1.58\ \text{fm}. \tag{16}$$

For ^{13}C, the parameters $(N, Z) = (7, 6)$, the 3 in Eq. (14) arises from the spin-angle function describing the $1p_{\frac{1}{2}}$ valence neutron, and the $f(q)$ is the form factor for the elementary nucleon [18]. Because ^{12}C and ^{13}C have root-mean-square radii which differ by only 0.02 fm [17], we took the parameters of the charge distribution of ^{12}C [17] as the proton parameters for ^{13}C parameters, and, there being no strong evidence to the contrary, we assume the parameters for the neutron and proton matter distributions are equal. In contrast, Hoffmann *et al.* [3] and Ray *et al.* [2] vary the neutron size to obtain a better fit the elastic p-^{12}C data.

The same assumptions for the form factors are made when we parametrize them with the Fermi or Wood-Saxon shape,

$$\rho(r) = \frac{\rho_0(1 - 0.149\, r^2/R^2)}{1 + e^{(r-R)/a}}, \tag{17}$$

$$(R, a, r_{\rm rms}) = (2.172, 0.5690, 2.38)\ \text{fm}. \tag{18}$$

We calculate the $\rho(q)$ by a numerical Fourier transform. First we determine the partial wave expansion of $\rho(q)$ at a large value of the momentum transfer $q = q_{\rm max} = 5.2\ \text{fm}^{-1} \stackrel{\rm def}{=} 2k_m$:

$$\rho(q) \simeq \sum_{l=0}^{48} \rho_l(k_m, k_m) P_l(1 - q^2/2k_m^2), \tag{19}$$

$$\rho_l(k_m, k_m) = 4\pi(2l+1) \int_0^\infty dr r^2 \rho(r) j_l(k_m) j_l(k_m)\ , \tag{20}$$

where we use 96 integration points in Eq. (20). The numerics were checked by reproducing over five decades the form factor published by Frosch *et al.* [19]. For momentum transfers larger than $q_{\rm max}$ we use an analytic expression which falls off exponentially in q^2 and which matches the magnitude and slope of our numeric one at $q_{\rm max}$:

$$\rho(q) = \rho(q_{\rm max}) e^{-(q^2 - q^2_{\rm max})/\alpha} \quad (q > q_{\rm max}). \tag{21}$$

Because there are no electron scattering measurements for these large values of q, Eq. (21) provides a well-behaved extrapolation with insignificant influence upon our computed cross sections. The off-energy-shell nucleon-nucleon T matrices (t) in the optical potential Eq. (10) are transformed to the p-^{13}C c.m. with a Lorentz covariant prescription, and an impulse approximation is made which optimizes the factorization approximation [15,16]:

$$t^{pN} = \langle \mathbf{k}', \mathbf{p}_0 - \mathbf{q}|\ t^{pN}(\omega[E])\ |\mathbf{k}, \mathbf{p}_0\rangle\,, \tag{22}$$

$$\mathbf{p}_0 = -\frac{\mathbf{k}}{A} + \frac{A-1}{2A}\,\mathbf{q}. \tag{23}$$

We take ω in Eq. (22) to be the "three-body energy,"

$$\omega^2 = \omega^2_{\rm 3B} = (k^\mu_p + k^\mu_A - P^\mu)^2, \tag{24}$$

$$P^2 \simeq \frac{A-1}{A}\left(k^2 + \frac{q^2}{4p_f^2} + \mathbf{q}\cdot\mathbf{k}\right), \quad p_f = 185\ \text{MeV}/c, \tag{25}$$

which clearly includes some recoil and binding effects into the first-order potential. This procedure leads to a different momentum and NN energy for each p-nucleus scattering angle.

The off-shell variation of the NN t matrices in each eigenchannel $\alpha = (JlS)$ is described with a separable potential,

$$\langle \kappa' |\, t_\alpha(\omega)\,|\, \kappa'\rangle = \frac{g_\alpha(\kappa')g_\alpha(\kappa)}{g^2_\alpha(\kappa_0)} \langle \kappa_0|\ t_\alpha(\omega)\,|\,\kappa_0\rangle\,, \tag{26}$$

where $\langle \kappa_0|\ t_\alpha(\omega)\,|\,\kappa_0\rangle$ is the on-shell amplitude determined from the phase-shift analyses of Arndt [20] (see Ref. [16] for a demonstration of the NN phase-shift sensitivity). We use the Graz NN potential [21] because its off-shell behavior closely approximates that of the Paris potential and provides consistent relativistic propagators in the two- and many-body systems. Because these elementary amplitudes are antisymmetrized, our optical potential inherently includes the exchange of the projectile and struck nucleon, but not with the other nucleons in the nucleus.

While not obvious from the form of the optical potential Eq. (10), the terms arising from the NN spin-orbit amplitude t_e, when converted to the standard form of Eq. (1), generate the V_e and V_f terms in the carbon potential:

$$V_e(\vec\sigma^p_n + \vec\sigma^C_n) + V_f(\vec\sigma^p_n - \vec\sigma^C_n) \equiv$$

$$N\left[t^{pn}_e \vec\sigma^p_n \rho^n_{\rm mt} + t^{pn}_e \vec\sigma^C_n \rho^n_{\rm sp}\right] + Z\left[t^{pp}_e \vec\sigma^p_n \rho^p_{\rm mt} + t^{pp}_e \vec\sigma^C_n\right], \tag{27}$$

and this implies

$$V_e = \frac{1}{2}\left[N t^{pn}_e(\rho^n_{\rm mt} + \rho^n_{\rm sp}) + Z t^{pp}_e(\rho^p_{\rm mt} + \rho^p_{\rm sp})\right], \tag{28}$$

$$V_f = \frac{1}{2}\left[N t^{pn}_e(\rho^n_{\rm mt} - \rho^n_{\rm sp}) + Z t^{pp}_e(\rho^p_{\rm mt} - \rho^p_{\rm sp})\right]. \tag{29}$$

Accordingly, V_f vanishes only if the distributions of neutron spin and neutron matter are the same, as well as the distributions of proton matter and spin (equalities not realized for ^{13}C).

IV. COUPLED-CHANNELS LIPPMANN-SCHWINGER EQUATION

Many-body effects and relativity leads to a potential V incorporating complicated nonlocalities. Rather than

treat such a potential in coordinate space and solve an integro-differential Schrödinger equation, we solve the Lippmann-Schwinger equation in momentum space:

$$T(\vec{k}',\vec{k}) = V(\vec{k}',\vec{k}) + \int \frac{d^3p}{E^+ - E(p)} V(\vec{k}',\vec{p})\, T(\vec{p},\vec{k}), \tag{30}$$

where $E(p) = E_p(p) + E_C(p)$ is the projectile plus target energy and the + superscript indicates a positive $i\epsilon$ has been added to the on-shell energy. To obtain one-dimensional integral equations, we expand T and V in spin-angle functions and substitute into this equation. A complication arises in our problem from the ability of the $V_f(\vec{\sigma}_n^p - \vec{\sigma}_n^C)$ term in the optical potential Eq. (11) to mix singlet and triplet states:

$$\langle 0,0|V|1,1\rangle = -\frac{i}{\sqrt{2}} V_f(\vec{k}',\vec{p}). \tag{31}$$

Accordingly, an extension of the phase-shift analysis used for NN scattering [6,7] is needed is given in the Appendix. We show there that the integral equations in the partial wave basis [14] have form:

$$\begin{bmatrix} T^{j(s_1s_1)}_{l_a l_a} \\ T^{j(s_2s_1)}_{l_b l_a} \end{bmatrix} = \begin{bmatrix} V^{j(s_1s_1)}_{l_a l_a} \\ V^{j(s_2s_1)}_{l_b l_a} \end{bmatrix} + \int_0^\infty \frac{p^2dp}{E^+ - E(p)} \begin{bmatrix} V^{j(s_1s_1)}_{l_a l_a}(k'p)\; V^{j(s_1s_2)}_{l_a l_b}(k',p) \\ V^{j(s_2s_1)}_{l_b l_a}(k',p)\; V^{j(s_2s_2)}_{l_b l_b}(k',p) \end{bmatrix} \begin{bmatrix} T^{j(s_1s_1)}_{l_a l_a}(p,k) \\ T^{j(s_2s_1)}_{l_b l_a}(p,k) \end{bmatrix}, \tag{32}$$

where we leave off the (k',k) dependence of the leftmost T's and V's, and use l, s, and j to denote the orbital, spin, and total angular momenta. We solve these equations on a grid of 40 momentum values for 48 angular momentum (l) values, which is large enough to avoid numerical noise.

The Vincent-Phatak technique for including the Coulomb potential in momentum-space calculations was formulated originally for uncoupled channels and low energies [22]. For the present calculation we have extended it [23] to coupled angular-momentum channels and to much larger numbers of partial waves and grid points. The Coulomb potential which we add to the optical potential is the Fourier transform of a potential arising from the actual nuclear charge distribution cutoff at some radius $R_{\rm cut}$:

$$V^{\rm cut}_{\rm Coul}(\mathbf{k}',\mathbf{k}) = \frac{Z_P Z_T e^2}{2\pi^2 q^2} \left[\rho(q) - \cos(qR_{\rm cut})\right]. \tag{33}$$

In the present calculations we take $R_{\rm cut} = 8$ fm, and have verified that our predictions are insensitive to a $1-2$ fm variation around this value. In this way the short-range nuclear force and the finite-range corrections to the Coulomb force are included directly in the Lippmann-Schwinger equation. The scattering from the point-Coulomb potential is included by adding the amplitude for scattering from a point-Coulomb potential $f^c_{\rm pt}$ to the a and b amplitudes:

$$\begin{pmatrix} a(\theta) \\ b(\theta) \end{pmatrix} \rightarrow \begin{pmatrix} a(\theta) + f^c_{\rm pt}(\theta) \\ b(\theta) + f^c_{\rm pt}(\theta) \end{pmatrix}. \tag{34}$$

V. RESULTS

The p-^{13}C experimental observables are determined by computing the a–f amplitudes and then substituting them into Eqs. (3)–(9). In trying to understand the

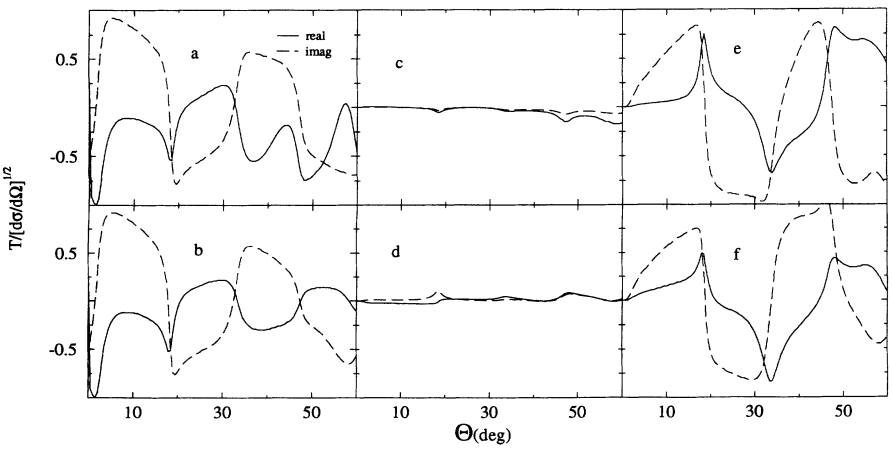

FIG. 1. The p-^{13}C spin amplitudes a–f of Eq. (1) as a function of scattering angle at 500 MeV. The amplitudes are divided by the square root of the differential cross sections to match the way they contribute to the spin observables in (3)–(9).

observables it is helpful to have a picture of the behavior of these p-^{13}C amplitudes as a function of scattering angle. We present such a picture in Fig. 1, where we set the scale by dividing the amplitudes by the square root of the cross section. Note that these amplitudes are for p-^{13}C, and accordingly have more oscillations and a greater falloff with momentum transfer than the elementary NN a–e amplitudes from which they derive.

We see in Fig. 1 that a and b are approximately equal in magnitude and in phase with each other, that e and f are also approximately equal in magnitude and in phase with each other, but that c and d are much smaller than the other amplitudes and of opposite phase to each other. Because the observables in Eqs. (3)–(9) are the sums of products of these amplitudes, we generally expect an observable to be large if it contains the product of two large amplitudes and to be small if it contains only c and d. However, the converse is not true, cancellation between large amplitudes can produce small values for an observable.

In Fig. 2 we compare the predicted cross sections to cross sections measured by Hoffmann *et al.* [3] at 500 MeV and by Seestrom-Morris *et al.* [1] at 547 MeV. We see that the theory produces good agreement with the forward peak of the 547 MeV data, is slightly too low for the 500 MeV data, and slightly too high for the larger-angle data. The locations of the minima and maxima in the 500 MeV data appear to be predicted well, which is important because the spin observables, being inversely proportional to $d\sigma/d\Omega$, are sensitive to the locations of these minima.

Although at first we believed the discrepancy in the 500 MeV forward differential cross sections showed the need to include Coulomb or channel coupling effects more correctly, the disagreement persists even with an exact treatment of the Coulomb force in a full coupled-channels formalism [23]. To see if the discrepancy is a size effect, in the top part of Fig. 3 we present predictions for $d\sigma/d\Omega$ using slightly smaller rms sizes (0.07 fm) and the harmonic oscillator form for the nuclear densities, Eqs. (12)–(16). We conclude that no simple size or shape change provides agreement with the forward peak of the 500 MeV data, and that there may be a small inconsistency between the 500 and 547 MeV data sets.

We have already indicated that a new aspect of the present study is its exact treatment of spin singlet-triplet coupling and the ensuing generation of the $f(\vec{\sigma}_n^p - \vec{\sigma}_n^C)$ term of the scattering amplitude Eq. (1). In Fig. 3 we show the importance of this f amplitude in the differential cross section (top) and analyzing power (bottom). As expected from Eq. (3), since the modulus squared of all amplitudes add to form $d\sigma/d\Omega$ (with four of the

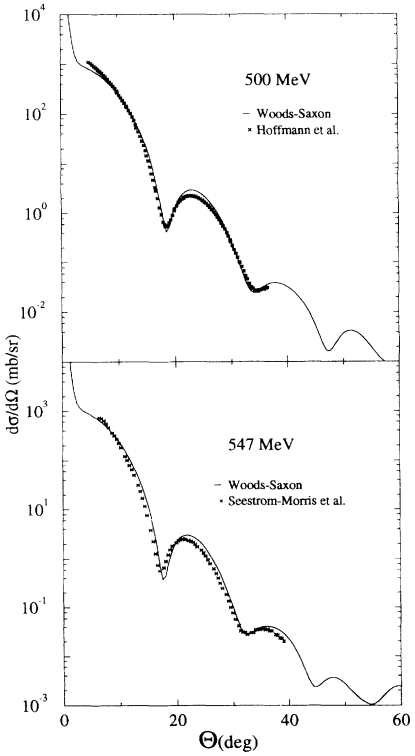

FIG. 2. Predictions for the p-^{13}C differential cross section at 500 MeV (top) and 547 MeV (bottom) compared, respectively, with the data of Hoffmann *et al.* [3] and Seestrom-Morris *et al.* [1]. The nucleus is described with the Wood-Saxon shape (17).

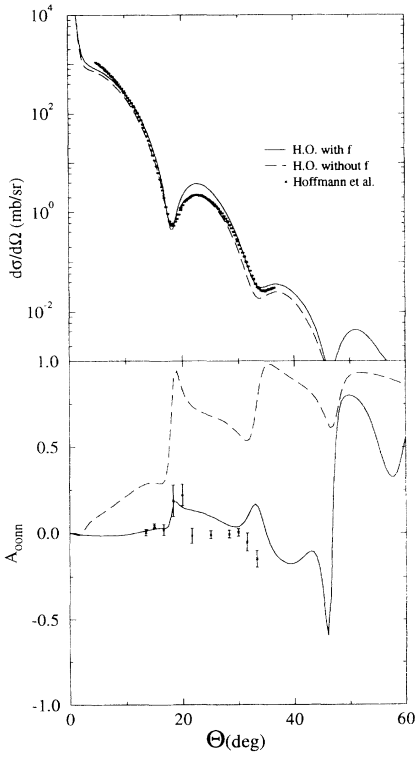

FIG. 3. The 500 MeV p-^{13}C differential cross section (top) and polarized target-polarized beam analyzing power $A_{oonn}^{(11)}$ (bottom) compared to the data of Hoffmann *et al.* [3]. The nucleus is described with the harmonic oscillator shape, (12)–(16). The dashed curves are the predictions with no f amplitude.

amplitudes being large), the f contribution is significant but not dominating. However, as may be expected from Eq. (9), since these same six amplitudes contribute to $A^{(11)}_{00nn}$ with cancellations (bottom of Fig. 3), f is more important there. Indeed, the dramatic improvement in the prediction of $A^{(11)}_{00nn}$ once f is included (bottom of Fig. 3) builds confidence in our treatment of the f term. However, the almost complete cancellation of amplitudes occurring in our prediction of $A^{(11)}_{00nn}$ (we are essentially predicting zero) warns that the spin observables may well be very sensitive to otherwise small effects in the theory.

In Fig. 4 we show predictions and data for the projectile analyzing power $A^{(2)}_{oono}$ (top) and the polarized target asymmetry $A^{(2')}_{ooon}$ (bottom). As we see from comparing the phenomenological forms Eqs. (4) and (5), $A^{(2),(2')}_{oono} \propto \mathrm{Re}(a^* e \pm b^* f)$, and so involve identical combinations of amplitudes with only the sign of the $b^* f$ term differing. The fact that the computed observables differ significantly indicates that the f amplitude is large. Further, as we see by comparing the top and bottom of Fig. 4, there is slightly too much *constructive* interference in the forward $A^{(2)}_{oono}$ and slightly too much *destructive* interference in the forward $A^{(2')}_{ooon}$. Because Fig. 1 shows that a and b tend to be in phase with each other, and that e and f tend to be in phase with each other, we suspect that our $a - e$ relative phase is not quite correct. In a non-coupled-channels spin $0 \times 1/2$ Schrödinger equation calculation, Arellano *et al.* [24] find a small forward peak in $A^{(2)}_{oono}$ when full Fermi average is performed; others [2], however, obtain good agreement without full folding but with the Dirac equation.

In the top part of Fig. 5 we compare theoretical and experimental values for the depolarization in the normal direction $D^{(3)}_{nono}$. The deviation of this observable from 1 measures spin-flip scattering which is interesting because it should be sensitive to the valence neutron in ^{13}C. However, as we see from its phenomenological form Eq. (6), all the large amplitude which enter into $D^{(3)}_{nono}$ are added together in moduli and then the small amplitudes are subtracted. Accordingly, and as is (all too) clear in the top part of Fig. 5, although our predictions for $D^{(3)}_{nono}$ agree well with the data, the small deviation from 1 renders the comparison nonrevealing.

In the middle and bottom parts of Fig. 5 we compare theoretical and experimental values for the sideways to longitudinal depolarization $D^{(4)}_{loso}$ and the sideways depolarization $D^{(5)}_{soso}$. Whereas the phenomenological forms for both observables, Eqs. (7) and (8), indicate they should be large in the forward direction, we see that $D^{(4)}_{loso}$ starts off with a strong destructive interference,

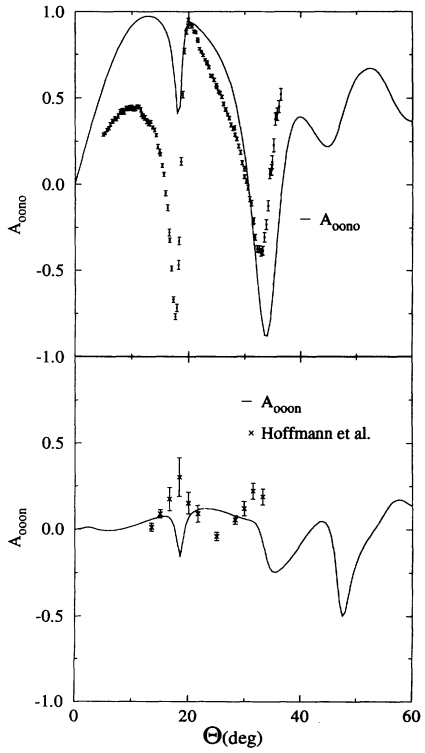

FIG. 4. The projectile analyzing power $A^{(2)}_{oono}$ (top), and the polarized target asymmetry $A^{(2')}_{ooon}$ (bottom), compared with the 500 MeV data of Hoffmann *et al.* [3].

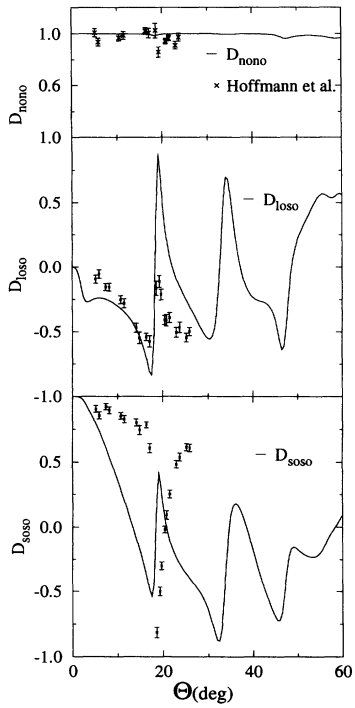

FIG. 5. The depolarization in the normal direction $D^{(3)}_{nono}$ (top), the sideways to longitudinal depolarization $D^{(4)}_{loso}$ (middle), and the sideways depolarization $D^{(5)}_{soso}$ (bottom) compared with the 500 MeV data of Hoffmann *et al.* [3].

while $D^{(5)}_{soso}$ commences with a strong constructive interference. As we see in Fig. 5, the theory does a very good job at predicting the sharp destructive interference in $D^{(4)}_{loso}$ (which also contains a large contribution from the f amplitude), but does not contain enough constructive interference for agreement with the forward part of $D^{(5)}_{soso}$ (although the location of the precipitous interference minimum in $D^{(5)}_{soso}$ is predicted accurately). Clearly, the relative phases of the amplitudes are important here.

VI. SUMMARY AND CONCLUSION

We have examined how well a first-order, theoretical optical potential can describe the cross sections and spin observables measured in elastic proton scattering from ^{13}C near 500 MeV. The theory includes the full spin dependences for two spin-1/2 particles, singlet-triplet mixing, nonlocalities arising from off-energy-shell behavior of the NN interaction, and Lorentz covariant, off-shell kinematics. When the resulting optical potential is used in a relativistic Schrödinger equation, multiple scattering and exchange effects are included.

These are our first results including the exact singlet-triplet mixing and the inclusion of the Coulomb force for coupled channels. We find that attaining agreement with the new data is quite a challenge. The theory is basically parameterless (we did however explore the sensitivity to nuclear size), and the spin observables are often the result of delicate interference between as many as six complex amplitudes, with slight variation of the amplitudes leading to significantly different predictions. To be expected, our agreement is not as good as that found in models whose parameters are adjusted to the ^{12}C data as a prerequisite to predicting ^{13}C [1–4,26]. Nevertheless, the level of agreement is comparable with that found by Arellano *et al.* [24] in a similar study of proton scattering from the simpler spin-0 light nuclei.

Clearly, improvements are needed and we believe the theory is advanced to the stage where they are worthwhile. We have omitted effects known to be important at lower energies such as nuclear correlations, virtual nuclear excitations, Pauli exclusion, and the density dependence of the effective interaction. Probably most important, our theory does not include effects known to be important at intermediate energies, namely, the negative energy degrees of freedom present in the Dirac equation [2,25–27], and the full folding over Fermi motion [24].

ACKNOWLEDGMENTS

We wish to thank Lanny Ray, Victor Madsen, Sid Coon, Otto Häuser, Charlie Drake, and Richard Woloshyn for stimulating and illuminating discussions. We also wish to gratefully acknowledge support from the U.S. Department of Energy under Grant DE-FG06-86ER40283. In addition, we wish to thank the people at the National Institute for Nuclear Theory, Seattle, and in the Physics Department of Melbourne University for their hospitality during part of this work.

APPENDIX: SPIN DECOMPOSITION

We extend the spin $1/2 \times 1/2$ phase-shift analysis [6,7] used for the NN problem in order to include the effect of the V_f potential's mixing of singlet and triplet states. We assume the conventional expansion of T and V in spin-angle functions:

$$V(\vec{k}',\vec{k}) = \frac{2}{\pi} \sum_{jm_j ll' ss'} i^{(l'-l)}\, V^{j(s's)}_{l'l}(k',k)\, \mathcal{Y}^{jm_j}_{l's'}(\hat{k}')\, \mathcal{Y}^{\dagger jm_j}_{ls}(\hat{k}), \tag{A1}$$

$$T(\vec{k}',\vec{k}) = \frac{2}{\pi} \sum_{jm_j ll' ss'} i^{(l'-l)}\, T^{j(s's)}_{l'l}(k',k)\, \mathcal{Y}^{jm_j}_{l's'}(\hat{k}')\, \mathcal{Y}^{\dagger jm_j}_{ls}(\hat{k}), \tag{A2}$$

where l, s, and j are the orbital, spin, and total angular momenta for the target plus projectile:

$$\vec{j} = \vec{l} + \vec{s}, \quad \vec{s} = \frac{1}{2}(\vec{\sigma^p} + \vec{\sigma^C}), \quad s = 0(s), 1(t). \tag{A3}$$

The $\mathcal{Y}$'s in Eqs. (A1) and (A2) are orthonormal spin-angle functions with the definition and properties [28]:

$$\mathcal{Y}^{jm}_{ls}(\hat{k}) = \sum_{m_s m_l} \langle l m_l s m_s | jm \rangle\, Y^{m_l}_l(\theta,\phi)\, |s m_s\rangle, \tag{A4}$$

$$Y^m_l(\theta,\phi) = (-1)^m \sqrt{\frac{(2l+1)(l-m)!}{4\pi(l+m)!}}\, P^m_l(\cos\theta) e^{im\phi}, \tag{A5}$$

$$P^m_l(x) = (1-x^2)^{m/2} \frac{d^m P_l(x)}{dx^m}. \tag{A6}$$

To evaluate the spin matrix elements, we adopt the Madison convention in which the z axis is taken as the beam direction $\vec{k}$ ($\phi_i = \theta_i = 0$), and the scattered momentum $\vec{k}'$ is placed in the xz plane ($\theta_f = \theta, \phi_f = 0$). We then follow

a two-step procedure in which we first evaluate [6] the potential Eq. (11) in the spin basis $|s, m_s\rangle$, and then invert the angular-momentum decomposition of the spin-basis matrix elements. The potential in the spin basis is

$$V_{s1}(\vec{k}',\vec{k}) \equiv \langle 0,0|V|1,1\rangle = -V_{1s}(\vec{k}',\vec{k}) = V_{s-1}(\vec{k}',\vec{k}) \;=\; \frac{-i}{\sqrt{2}} V_f(\vec{k}',\vec{k}), \tag{A7}$$

$$\begin{aligned} V_{ss}(\vec{k}',\vec{k}) &\equiv \langle 0,0|V|0,0\rangle \\ &= V_{a+b}(\vec{k}',\vec{k}) - V_{a-b}(\vec{k}',\vec{k}) - V_{c+d}(\vec{k}',\vec{k}) - V_{c-d}(\vec{k}',\vec{k}), \end{aligned} \tag{A8}$$

$$\begin{aligned} V_{00}(\vec{k}',\vec{k}) &\equiv \langle 1,0|V|1,0\rangle \\ &= V_{a+b}(\vec{k}',\vec{k}) + V_{a-b}(\vec{k}',\vec{k}) + \Big(V_{c+d}(\vec{k}',\vec{k}) - V_{c-d}(\vec{k}',\vec{k})\Big)\cos\theta, \end{aligned} \tag{A9}$$

$$V_{11}(\vec{k}',\vec{k}) = V_{-1-1} = V_{a+b}(\vec{k}',\vec{k}) + V_{c+d}(\vec{k}',\vec{k})\sin^2\frac{\theta}{2} + V_{c-d}(\vec{k}',\vec{k})\cos^2\frac{\theta}{2}, \tag{A10}$$

$$\begin{aligned} V_{10}(\vec{k}',\vec{k}) &= -V_{-10} \\ &= \frac{-i}{\sqrt{2}} V_e(\vec{k}',\vec{k}) - \frac{1}{\sqrt{2}} V_{c+d}(\vec{k}',\vec{k})\sin\theta + \frac{1}{\sqrt{2}} V_{c-d}(\vec{k}',\vec{k})\sin\theta, \end{aligned} \tag{A11}$$

$$\begin{aligned} V_{01}(\vec{k}',\vec{k}) &= -V_{0-1} \\ &= \frac{i}{\sqrt{2}} V_e(\vec{k}',\vec{k}) - \frac{1}{\sqrt{2}} V_{c+d}(\vec{k}',\vec{k})\sin\theta + \frac{1}{\sqrt{2}} V_{c-d}(\vec{k}',\vec{k})\sin\theta, \end{aligned} \tag{A12}$$

$$V_{1,-1}(\vec{k}',\vec{k}) = V_{-11} = -V_{a-b}(\vec{k}',\vec{k}) + V_{c+d}(\vec{k}',\vec{k})\cos^2\frac{\theta}{2} + V_{c-d}(\vec{k}',\vec{k})\sin^2\frac{\theta}{2}. \tag{A13}$$

Next we expand the spin matrix elements in angular-momentum states:

$$\begin{aligned} \langle s'''m_s'''|V(\vec{k}',\vec{k})|s''m_s''\rangle = \frac{2}{\pi} \sum_{js'sl'lm_sm_{s'}m_lm_{l'}} & \langle s'''m_s'''|s'm_s'\rangle\, i^{l-l'}\, \langle l'm_l's'm_s'|jm\rangle \\ & \times \langle jm|lm_lsm_s\rangle Y_{l'}^{m_{l'}}(\theta_f,\phi_f)\, V_{l'l}^{js's}(k',k)\, Y_l^{m_l^*}(\theta_i,\phi_i)\, \langle sm_s|s'',m_s''\rangle, \end{aligned} \tag{A14}$$

where (k,θ_i,ϕ_i) and (k',θ_f,ϕ_f) are the spherical coordinates of the initial and final momenta. The Clebsch-Gordan coefficients vanish unless $l = l' \pm 1, l'$ and $m_j = m_l + m_s = m_l' + m_s'$, and parity conservation requires $|l - l'| = 0, 2$. In the Madison convention the projectile has no angular momentum in its propagation direction and so $m_l = 0$, in which case

$$Y_l^{m_l^*}(\theta_i,\phi_i) = Y_l^0(0,0) = \sqrt{\frac{2l+1}{4\pi}}. \tag{A15}$$

As an example we consider the V_{s1} term Eq. (A7) which couples the singlet state to the triplet state. Because j is a constant and $s' = 0$ in the final state, the total angular momentum j must equal l'. Parity conservation requires $l = l'$, and because m_s and m_l are 1 and 0, we must have $m_j = 1$, and $m_{l'} = 1$. The sum in Eq. (A14) then reduces to a simple sum in the final orbital angular momentum l'. In this way we obtain the partial wave decompositions:

$$V_{s1}(\vec{k}',\vec{k}) = \frac{-\sqrt{2}}{4\pi^2} \sum_{l=1} P_l^1(x = \cos\theta_{k'k}) \frac{2l+1}{\sqrt{l(l+1)}} V_{ll}^{l(st)}(k',k), \tag{A16}$$

$$V_{ss}(\vec{k}',\vec{k}) = \frac{1}{2\pi^2} \sum_{l=0} P_l(x)(2l+1)\, V_{ll}^{l(ss)}(k',k), \tag{A17}$$

$$\begin{aligned} V_{11}(\vec{k}',\vec{k}) = \frac{1}{4\pi^2} \sum_{l=0} P_l(x) \Big\{ & (l+2) V_{ll}^{l+1(tt)}(k',k) - \sqrt{(l+1)(l+2)}\, V_{ll+2}^{l+1(tt)}(k',k) \\ & + (2l+1) V_{ll}^{l(tt)}(k',k) + (l-1) V_{ll}^{l-1(tt)}(k',k) - \sqrt{(l-1)l}\, V_{ll-2}^{l-1(tt)}(k',k) \Big\}, \end{aligned} \tag{A18}$$

$$\begin{aligned} V_{00}(\vec{k}',\vec{k}) = \frac{1}{2\pi^2} \sum_{l=0} P_l(x) \Big\{ & (l+1) V_{ll}^{l+1(tt)}(k',k) + l V_{ll}^{l-1(tt)}(k',k) \\ & + \sqrt{(l+1)(l+2)}\, V_{ll+2}^{l+1(tt)}(k',k) + \sqrt{(l-1)l}\, V_{ll-2}^{l-1(tt)}(k',k) \Big\}, \end{aligned} \tag{A19}$$

$$V_{10}(\vec{k}',\vec{k}) = \frac{\sqrt{2}}{4\pi^2}\sum_{l=1} P_l^1(x)\left\{-V_{ll}^{l-1(tt)}(k',k)+V_{ll}^{l+1(tt)}(k',k) + \sqrt{\frac{l+2}{l+1}}V_{ll+2}^{l+1(tt)}(k',k) - \sqrt{\frac{l-1}{l}}V_{ll-2}^{l-1(tt)}(k',k)\right\}, \tag{A20}$$

$$V_{01}(\vec{k}',\vec{k}) = \frac{\sqrt{2}}{4\pi^2}\sum_{l=1} P_l^1(x)\left\{-\frac{l+2}{l+1}V_{ll}^{l+1(tt)}(k',k) + \frac{2l+1}{l(l+1)}V_{ll}^{l(tt)}(k',k) + \frac{l-1}{l}V_{ll}^{l-1(tt)}(k',k) + \sqrt{\frac{l+2}{l+1}}V_{ll+2}^{l+1(tt)}(k',k) - \sqrt{\frac{l-1}{l}}V_{ll-2}^{l-1(tt)}(k',k)\right\}, \tag{A21}$$

$$V_{1\,-1}(\vec{k}',\vec{k}) = \frac{1}{4\pi^2}\sum_{l=2} P_l^2(x)\left\{\frac{1}{l+1}V_{ll}^{l+1(tt)}(k',k) - \frac{1}{\sqrt{(l+1)(l+2)}}V_{ll+2}^{l+1(tt)}(k',k) - \frac{2l+1}{l(l+1)}V_{ll}^{l(tt)}(k',k) + \frac{1}{l}V_{ll}^{l-1(tt)}(k',k) - \frac{1}{\sqrt{l(l-1)}}V_{ll-2}^{l-1(tt)}(k',k)\right\}. \tag{A22}$$

Note that the sums are over the orbital angular momentum of the final state, and that we have combined matrix elements of different j values if they multiply the same Legendre polynomial (the Lippmann-Schwinger equations couple states with the same j only).

We invert Eqs. (A16)–(A22) for the partial wave potentials $V_{l'l}^{j(s's)}(k',k)$ by multipling the equation for each $V_{m'm}$ by $P_l^{|m'-m|}$, and numerically evaluating the integral:

$$I_{m'm}(k',k) = \int_{-1}^{1} dx\, V_{m'm}(\vec{k}',\vec{k})\, P_l^{|m'-m|}(\cos\theta_{k'k}). \tag{A23}$$

For Eq. (A16) and Eq. (A17) the inversion is simple because only one $V_{l'l}^{j(s's)}$ is involved:

$$V_{ll}^{l(st)}(k',k) = V_{ll}^{l(ts)}(k',k) = \frac{-\sqrt{2}\pi^2}{\sqrt{l(l+1)}}I_{s1}(k',k), \tag{A24}$$

$$V_{ll}^{l(ss)}(k',k) = \pi^2 I_{ss}(k',k). \tag{A25}$$

Equations (A18)–(A22) contain $V_{l'l}^{j(tt)}$'s intermixed for differing j and l values, and so the projection results in five coupled equations:

$$\vec{I} = B\vec{V}, \tag{A26}$$

$$\begin{pmatrix} I_{11}(k',k) \\ I_{00}(k',k) \\ I_{10}(k',k) \\ I_{01}(k',k) \\ I_{1-1}(k',k) \end{pmatrix} = \begin{pmatrix} \\ B_{l'l}^{m'm} \\ \\ \end{pmatrix} \begin{pmatrix} V_{ll}^{l+1(tt)}(\vec{k}',\vec{k}) \\ V_{ll}^{l(tt)}(\vec{k}',\vec{k}) \\ V_{ll}^{l-1(tt)}(\vec{k}',\vec{k}) \\ V_{ll+2}^{l+1(tt)}(\vec{k}',\vec{k}) \\ V_{ll-2}^{l-1(tt)}(\vec{k}',\vec{k}) \end{pmatrix}, \tag{A27}$$

where $B_{l'l}^{m'm}$ makes up a matrix of coefficients multiplying the V's in Eqs. (A18)–(A22). We solve the matrix equation (A27) by matrix inversion,

$$\vec{V} = B^{-1}\vec{I}. \tag{A28}$$

Finally, we check the procedure by recombining the potential according to Eqs. (A16)–(A22) and comparing to the original.

The substitution of the partial wave expansions into the three-dimensional Lippmann-Schwinger equation leads to the coupled integral equations:

$$\begin{bmatrix} T_{jj}^{j(ss)} \\ T_{jj}^{j(ts)} \end{bmatrix} = \begin{bmatrix} V_{jj}^{j(ss)} \\ V_{jj}^{j(ts)} \end{bmatrix} + \int_0^\infty \frac{p^2dp}{E^+ - E(p)} \begin{bmatrix} V_{jj}^{j(ss)}(k',p)\; V_{jj}^{j(st)}(k',p) \\ V_{jj}^{j(ts)}(k',p)\; V_{jj}^{j(tt)}(k',p) \end{bmatrix} \begin{bmatrix} T_{jj}^{j(ss)}(p,k) \\ T_{jj}^{j(ts)}(p,k) \end{bmatrix}, \tag{A29}$$

$$\begin{bmatrix} T_{jj}^{j(tt)} \\ T_{jj}^{j(st)} \end{bmatrix} = \begin{bmatrix} V_{jj}^{j(tt)} \\ V_{jj}^{j(st)} \end{bmatrix} + \int_0^\infty \frac{p^2dp}{E^+ - E(p)} \begin{bmatrix} V_{jj}^{j(tt)}(k',p)\; V_{jj}^{j(ts)}(k',p) \\ V_{jj}^{j(st)}(k',p)\; V_{jj}^{j(ss)}(k',p) \end{bmatrix} \begin{bmatrix} T_{jj}^{j(tt)}(p,k) \\ T_{jj}^{j(st)}(p,k) \end{bmatrix}, \tag{A30}$$

$$\begin{bmatrix} T_{j-1j-1}^{j(tt)} \\ T_{j+1j-1}^{j(tt)} \end{bmatrix} = \begin{bmatrix} V_{j-1j-1}^{j(tt)} \\ V_{j+1j-1}^{j(tt)} \end{bmatrix} + \int_0^\infty \frac{p^2dp}{E^+ - E(p)} \begin{bmatrix} V_{j-1j-1}^{j(tt)}(k',p)\; V_{j-1j+1}^{j(tt)}(k',p) \\ V_{j+1j-1}^{j(tt)}(k',p)\; V_{j+1j+1}^{j(tt)}(k',p) \end{bmatrix} \begin{bmatrix} T_{j-1j-1}^{j(tt)}(p,k) \\ T_{j+1j-1}^{j(tt)}(p,k) \end{bmatrix}, \tag{A31}$$

$$\begin{bmatrix} T_{j+1j+1}^{j(tt)} \\ T_{j-1j+1}^{j(tt)} \end{bmatrix} = \begin{bmatrix} V_{j+1j+1}^{j(tt)} \\ V_{j-1j+1}^{j(tt)} \end{bmatrix} + \int_0^\infty \frac{p^2dp}{E^+ - E(p)} \begin{bmatrix} V_{j+1j+1}^{j(tt)}(k',p)\; V_{j+1j-1}^{j(tt)}(k',p) \\ V_{j-1j+1}^{j(tt)}(k',p)\; V_{j-1j-1}^{j(tt)}(k',p) \end{bmatrix} \begin{bmatrix} T_{j+1j+1}^{j(tt)}(p,k) \\ T_{j-1j+1}^{j(tt)}(p,k) \end{bmatrix}. \tag{A32}$$

TABLE I. Notations for spin $1/2 \times 1/2$ amplitudes.[a]

$T_{l\,l'}^{j(ss')}$	$T_{j\,j}^{j(ss)}$	$T_{j\,j}^{j(ts)}$	$T_{j-1\,j-1}^{j(tt)}$	$T_{j+1\,j-1}^{j(tt)}$	$T_{j+1\,j+1}^{j(tt)}$	$T_{j-1\,j+1}^{j(tt)}$	$T_{j\,j}^{j(tt)}$	$T_{j\,j}^{j(st)}$
Spin	0	$1 \leftarrow 0$	1	1	1	1	1	$0 \leftarrow 1$
Δl	0	0	0	2	0	-2	0	0
Stapp	α_l	–	$\alpha_{l,l+1}$	α^{l-1}	$\alpha_{l,l-1}$	α^{l+1}	α_{ll}	–
$N_{\rm spin}$	1	2	3	4	5	6	7	8

[a] $T_{0\,0}^{0(tt)} = T_{-1\,-1}^{0(tt)} = T_{1\,-1}^{0(tt)} = T_{-1\,1}^{0(tt)} = 0$.

Equations (A29) and (A30) describe singlet-triplet coupling arising from the V_f term in the optical potential Eq. (11), which in turn produces an f term in the scattering amplitude Eq. (1). Equations (A31) and (A32) describe mixing within the triplet state arising from the tensor-force terms $V_{a-b}, V_{c+d}, V_{c-d}$ in the potential Eq. (11). Because the total angular momentum j is a conserved quantity, all coupled states have the same j superscript.

Once the $T_{l'l}^{j(s's)}$'s have been solved for, the matrix elements in the spin basis $\langle s' m_{s'} | T | s m_s \rangle$ are computed via Eqs. (A16)–(A22) with the V's replaced by T's. The $a-f$ amplitudes are then

$$a = \frac{1}{2}\left(T_{11} + T_{00} - T_{1-1}\right), \tag{A33}$$

$$b = \frac{1}{2}\left(T_{11} + T_{ss} + T_{1-1}\right), \tag{A34}$$

$$c = \frac{1}{2}\left(T_{11} - T_{ss} + T_{1-1}\right), \tag{A35}$$

$$d = \frac{1}{2}\left(T_{00} + T_{1-1} - T_{11}\right)/(2\cos\theta_{kk}) \tag{A36}$$

$$= -\left(T_{10} + T_{01}\right)/(\sqrt{2}\sin\theta_{k'k}), \tag{A37}$$

$$e = \frac{i}{\sqrt{2}}\left(T_{10} - T_{01}\right), \tag{A38}$$

$$f = i\sqrt{2}T_{s1}. \tag{A39}$$

The on-energy-shell T matrix elements in the partial wave basis are related to the bar phase shifts [8,7]:

$$-2i\rho T_{j\,j}^{j(ss)}(k_0,k_0) = \cos 2\bar{\gamma}_l e^{2i\bar{\delta}_j} - 1, \tag{A40}$$

$$-2i\rho T_{j\,j}^{j(tt)}(k_0,k_0) = \cos 2\bar{\gamma}_l e^{2i\bar{\delta}_{jj}} - 1, \tag{A41}$$

$$-2i\rho T_{j\pm1\,j\pm1}^{j\ (tt)}(k_0,k_0) = \cos 2\bar{\epsilon}_j e^{2i\bar{\delta}_{j\pm1\,j}} - 1, \tag{A42}$$

$$-2i\rho T_{j\pm1\,j\mp1}^{j\ (tt)}(k_0,k_0) = -i\sin 2\bar{\epsilon}_j\, e^{i(\bar{\delta}_{j-1\,j}+\bar{\delta}_{j+1\,j})}, \tag{A43}$$

$$-2i\rho T_{j\,j}^{j(ts)}(k_0,k_0) = -i\sin 2\bar{\gamma}_l\, e^{i(\bar{\delta}_j+\bar{\delta}_{jj})}, \tag{A44}$$

$$\rho = 2k_0 \frac{E_p(k_0)E_t(k_0)}{E_p(k_0)+E_t(k_0)}, \tag{A45}$$

where the parameter $\bar{\gamma}_l$ is the mixing angle between the $|0,0\rangle$ singlet and $|1,1\rangle$ triplet state and the parameter $\bar{\epsilon}_l$ is the mixing angle between the l and $l+2$ triplet states. In Table I we give the connection to the α notation of Stapp [7] and the $N_{\rm spin}$ notation used in our computer code *Lpotp2*.

[1] S.J. Seestrom-Morris, M.A. Franey, D. Dehnhard, D.B. Holtkamp, R.L. Bourdie, J.F. Amann, G.C. Idzorek, and C.A. Goulding, Phys. Rev. C **30**, 270 (1984).

[2] L. Ray, G.W. Hoffmann, M.L. Barlett, J.D. Lumpe, B.C. Clark, S. Hama, and R.L. Mercer, Phys. Rev. C **37**, 1169 (1988).

[3] G.W. Hoffmann, M.L. Barlett, D. Ciskowski, G. Pauletta, M. Purcell, L. Ray, J.F. Amann, J.J. Jarmer, K.W. Jones, S. Penttilä, N. Tanaka, M.M.Gazzaly, J.R. Comfort, B.C. Clark, and S. Hama, Phys. Rev. C **41**, 1651 (1990).

[4] G.W. Hoffmann, M.L. Barlett, W. Kielhorn, G. Pauletta, M. Purcell, L. Ray, J.F. Amann, J.J. Jarmer, K.W. Jones, S. Penttilä, N. Tanaka, G. Burleson, J. Faucett, M. Gilani, G. Kyle, L. Stevens, A.M. Mack, D. Mihailidis, T. Averett, J. Comfort, J. Görgen, J. Tinsley, B.C. Clark, S. Hama, and R.L. Mercer, Phys. Rev. Lett. **65**, 3096 (1990).

[5] G.R. Goldstein and M.J. Moravcsik, Ann. Phys. (N.Y.) **142**, 219 (1982).

[6] M. Goldberger and K. Watson *Collision Theory* (Wiley, New York, 1964).

[7] H.P. Stapp, T.J. Ypsilantis, and N. Metropolis, Phys. Rev. **105**, 302 (1957).

[8] A. Gersten, Phys. Rev. C **18**, 2252 (1978); **24**, 2174 (1981).

[9] A.G. Williams, A.W. Thomas, and G.A. Miller, Phys. Rev. C **36**, 1956 (1987).

[10] J. Bystricky, F. Lehar, and P. Winternitz, J. Phys. (Paris) **39**, 1 (1978).

[11] P. La France and P. Winternitz, J. Phys. (Paris) **41**, 1391 (1980); correction in [2].

[12] P.L. Csonka, Rev. Mod. Phys. **37**, 177 (1965).

[13] R.H. Landau, M. Sagen, and G. He, Phys. Rev. C **41**, 50 (1990).

[14] Although neither T nor V is a wave, we refer to their angular momentum decomposition as a "partial wave" expansion.

[15] M.J. Paez and R. H. Landau, Phys. Rev. C **29**, 2267 (1984); **30**, 1757 (1984); Phys. Lett. **142B**, 235 (1984).

[16] R.H. Landau and M. Sagen, Phys. Rev. C **33**, 447 (1986).

[17] C.W. DeJager, H. DeVries, and C. DeVries, At. Data Nucl. Data Tables **14**, 479 (1974).

[18] B.Bartoli, F. Felicetti, and V.S. Silvestrini, Rev. Nuovo Cimento **2**, 241 (1972).

[19] R.F. Frosch, R. Hofstadter, J.S. McCarthy, G.K. Nöldeke, K.J. vanOostrum, M.R. Yearian, B.C. Clark, R. Herman, and D.G. Ravenhall, Phys. Rev. **174**, 1380 (1968).

[20] R.A. Arndt, L.D. Roper, R.A. Bryan, R.B. Clark, B.J. VerWest, and P. Signell, SAID dial up system, IP no. 128.173.176.61, userid=physics, password=quantum.

[21] K. Schwarz, J. Haidenbauer, and J. Frohlich, Phys. Rev. C **86**, 456 (1986).
[22] C.M. Vincent and S.C. Phatak, Phys. Rev. **10**, 391 (1974).
[23] D. Lu, T. Mefford, G. Song, and R.H. Landau, *Coulomb Plus Nuclear Scattering in Momentum Space for Coupled Angular-Momentum States*, OSU Report No. 94-6, 1994.
[24] H.F. Arellano, F.A. Brieva, and W.G. Love, Phys. Rev. C **41**, 2188 (1990); H.F. Arellano, F.A. Brieva, W.G. Love, and K. Nakayama, *ibid.* **43**, 1875 (1991).
[25] L. Ray, Phys. Rev. C **41**, 2816 (1990).
[26] L. Ray, Phys. Rev. C **47**, 2990 (1993).
[27] B.C. Clark, in *Relativstic Dynamics and Quark-Nuclear Physics*, edited by M.B. Johnson and A. Pickelseimer (Wiley, New York, 1986), p. 302.
[28] This is the sign convention of Messiah and Goldberger and Watson. It differs by $(-1)^m$ from Abrahmowitz and Stegun, Jackson, and some unpublished work of Goddard.